International Journal of Radiation Biology, August 2013; 89(8): 611–617

ISSN 0955-3002 print / ISSN 1362-3095 online
DOI: 10.3109/09553002.2013.782446

informa
healthcare

Microlocalization of lipophilic porphyrins: Non-toxic enhancers of boron neutron-capture therapy

Henry M. Smilowitz[1]*, Daniel N. Slatkin[2], Peggy L. Micca[2] & Michiko Miura[2]*

[1]*Department of Cell Biology, University of Connecticut Health Center, Farmington, Connecticut, and* [2]*Biosciences Department, Brookhaven National Laboratory, Upton, New York, USA*

Abstract

Purpose: **To compare the macroscopic and microscopic distributions of the novel non-toxic lipophilic porphyrins copper (II) 5,10,15,20-tetrakis-(3-[1,2 dicarba-*closo*-dodecaboranyl]methoxyphenyl)-porphyrin (CuTCPH), potentially useful for boron neutron-capture therapy (BNCT), with those of its zinc fluorescent congener zinc (II) 5,10,15,20-tetrakis-(3-[1,2 dicarba-*closo*-dodecaboranyl]methoxyphenyl)-porphyrin (ZnTCPH) in tissues of tumor-bearing mice.**

***Materials and methods*: ZnTCPH and CuTCPH were synthesized, then injected intraperitoneally (ip) into tumor-bearing mice. Macroscopic biodistribution was assessed by determining average boron concentrations in tumor, blood, brain, skin, and liver using atomic-emission spectrometry. The euthanized mice and their vital organs were photographed first under an ultraviolet lamp and then under a bright fluorescent lamp. Thin sections of liver and tumor were analyzed by confocal fluorescence microscopy (CFM).**

Results: **ZnTCPH-injected, but not CuTCPH-injected mice bearing subcutaneous tumors showed fluorescence from liver, spleen and tumors. Macrodistributions of boron in various tissues were similar in mice whether injected with ZnTCPH or CuTCPH. CFM of unfixed liver sections showed cytoplasmic fluorescence from Kupffer cells in a periportal lobular distribution evenly throughout the liver. In the tumors studied, such fluorescence was also cytoplasmic but unlike liver fluorescence, was macroscopically heterogeneous.**

Conclusion: **ZnTCPH serves as a useful fluorescent experimental surrogate for CuTCPH to delineate its macroscopic and microscopic distributions in organs and tumors.**

Keywords: Porphyrins, carborane, confocal microscopy, BNCT

Introduction

Boron neutron-capture therapy (BNCT) is a form of radiosurgery implemented by parenteral administration of one or more boron-rich agents (synthesized with >95 atom % ^{10}B; $>95\%$ of boron atoms are ^{10}B and 5% are ^{11}B) that accumulate preferentially in the tumor, followed by irradiation of the tumor-bearing zone with slow neutrons (Coderre and Morris 1999, Barth et al. 2012). In Japan, the USA, Argentina, and several European countries, BNCT has been used with water-soluble ^{10}B-enriched agents, notably p-boronophenylalanine (BPA) and/or sodium mercaptoundecahydrododecaborane (BSH) to palliate several types of human malignancies (Haritz et al. 1994, Chanana et al. 1999, Joensuu et al. 2003, Henriksson et al. 2008, Yamamoto et al. 2008, Sköld et al. 2010, Kawabata et al. 2011a, Kankaanranta et al. 2012). Infusions of BPA in glioblastoma patients yielded average tumor boron concentrations up to ~3–4 times greater than those concomitantly in the blood (Joel et al. 1997, Cruickshank et al. 2009). Average tumor boron concentrations achieved with nontoxic lipophilic porphyrins are generally one order of magnitude greater than those achievable with BPA or BSH (Miura et al. 1996, 1998, Renner et al. 2006). After intravenous (iv) injection, such porphyrins accumulate and remain for days at therapeutically relevant concentrations in several types of animal tumors. They also accumulate robustly in several normal organs, notably the liver, but are virtually excluded from normal brain tissues and are cleared from the blood (Miura et al. 1998, 2004). Copper (II) 5,10,15,20-tetrakis-(3-[1,2 dicarba-*closo*-dodecaboranyl]methoxyphenyl)-porphyrin (CuTCPH) (Miura et al. 2001) and its octabromo analogue, copper (II) 2,3,7,8,12,13,17,18-octabromo-5,10,15,20-tetrakis(3-[1,2-dicarba-*closo*-dodecaboranyl]methoxyphenyl)-porphyrin, (CuTCPBr) (Miura et al. 2004, 2012) are lipophilic congeners that can deliver robust concentrations of boron to several subcutaneous (sc) malignancies in mice with minimal toxicity. The subcutaneous (sc) murine EMT-6 mammary carcinoma has been palliated effectively by CuTCPH-based BNCT (Miura et al. 2001) and by CuTCPBr-enhanced X-ray radiotherapy (Miura et al. 2012). CuTCPBr or CuTCPH could also be used to image tumors noninvasively by labeling with ^{67}Cu for single-photon emission computed tomography (SPECT) or with ^{64}Cu for positron-emission tomography (PET). The

*HMS and MM made equal contributions to this paper.

Correspondence: Dr Henry M. Smilowitz, PhD, Department of Cell Biology; University of Connecticut Health Center; 263 Farmington Avenue; Farmington, CT 06030, USA. Tel: + 1 (860) 679 2710. Fax: + 1 (860) 679 3693. E-mail: Smilowitz@nso1.uchc.edu

(Received 11 June 2012; revised 20 February 2013; accepted 21 February 2013)

former may also be employed for tissue-localization studies by autoradiography using dental X-ray films (M. Miura, unpublished observations).

The microdistribution of a ^{10}B carrier is a major determinant of its effectiveness for BNCT; ^{10}B is roughly three-fold more efficient in the nucleus than in the cytoplasm (Gabel et al. 1987). The macrodistributions of a number of water-soluble porphyrins that localize in tumors of rodents have been studied previously (Ozawa et al. 2005, Fabris et al. 2007) and the microlocalization of a water-soluble porphyrin was studied in vitro (Fabris et al. 2007), but to our knowledge the microlocalization of a boron-containing lipophilic porphyrin in any tumor has not been reported.

In order to study microlocalization properties of non-fluorescent CuTCPH by confocal fluorescence microscopy (CFM) of tissues in vivo, we synthesized a fluorescent congener by replacing the copper (II) with zinc (II) to form zinc (II) 5,10,15,20-tetrakis-(3-[1,2 dicarba-*closo*-dodecaboranyl] methoxyphenyl)-porphyrin (ZnTCPH); zinc (II) porphyrins are fluorescent and copper (II) porphyrins are not, due mainly to the differences between the number of d electrons of those metals (Hopf and Whitten 1975). We then investigated its cellular and subcellular distributions in tumors and livers from mice using CFM, a technique employed for analogous studies related to photodynamic therapy (PDT) (Woodburn et al. 1991). Skin photosensitization by ZnTCPH contraindicates its clinical use, but CuTCPH merits study as a candidate enhancer of clinical boron neutron-capture therapy. It is possible that CFM information from ZnTCPH employed here as a fluorescent surrogate for CuTCPH in pre-clinical investigations might better enable treatment planning for pre-clinical studies of CuTCPH-mediated BNCT.

Materials and methods

Chemistry

All chemicals used for the synthesis of porphyrins and their formulations were purchased from Sigma-Aldrich (St Louis, MO, USA). CuTCPH was synthesized as described (Miura et al. 2001). Briefly, Cu (II) acetate (~1.5 mole equivalent) in methanol was added into a solution of free base porphyrin in dichloromethane for ~1 h at ambient temperature and monitored by optical spectroscopy (Carey 50 Spectrophotometer, Varian Inc., Palo Alto, CA, USA). The product was diluted with dichloromethane, washed with water, its solvents evaporated, and the residue purified by flash chromatography using silica and 1:1 hexanes:dichloromethane as eluent. Substitution of Zn (II) acetate for Cu (II) acetate in the same procedure yielded ZnTCPH. These metalloporphyrins were generally obtained in $>$90% yield from the free-base starting material.

Preparation of porphyrin solution for injection

A ~3 milligram (mg)/milliliter (ml) porphyrin solution in 9% Cremophor EL (CRM) (currently called Kalliphor EL, BASF Corp., Ludwigshafen, Germany) and 18% propylene glycol (PRG) was prepared by dissolving the porphyrin in tetrahydrofuran (THF) (1.5% of the total volume), then heating the solution at 40°C for ~15 min. CRM (9% of total volume) was added and the mixture was heated to 60°C for 2 h, evaporating virtually all the THF. After cooling to room temperature, PRG (18% of total volume) was added, followed by dropwise addition of saline (71.5% of total volume) with rapid stirring. The resultant formulation, a CRM/PRG emulsion, was degassed by stirring under vacuum (~30 mm Hg) for 30–60 min then filtered (Millipore, 8 µm, Billerica, MA, USA) (Zuk et al. 1994, Miura et al. 2001). The CRM excipient used for these studies is stable, non-toxic and effects high delivery of porphyrin to tumors in vivo. It has been used by us for many years for pre-clinical studies of our lipophilic porphyrins. A more recently developed formulation consisting of 2% purified Cremophor EL (ELP), 1% Tween 80, 5% ethanol and 2.2% PEG 400, designated the CTEP formulation (Miura et al. 2012), was not available when these studies were performed.

Tumor models

One human and two murine tumor cell lines were grown in Dulbecco's Modified Eagle Medium (DMEM)-enriched medium with 10% fetal bovine serum, 1% penicillin/streptomycin, and 1% L-glutamine. The two murine malignancies were studied by CFM as sc leg tumors. The EMT-6 mouse mammary tumor cell line kindly provided by Dr Rockwell (Rockwell et al. 1972) was initially grown sc to at least 100 mm^3 in the dorsal thorax of isogeneic female BALB/c mice (20–25 g, Taconic Farms, Germantown, NY, USA). Freshly removed primary tumor tissue was then minced in saline and $<$0.5 mm fragments were implanted sc in the legs of female BALB/c mice through an 18-gauge trocar (Miura et al. 2001). Murine SCCVII squamous cell carcinoma cells (5×10^5) (kindly provided by Prof. J. Martin Brown, Stanford University) were grown similarly in the dorsal thorax and implanted sc in the legs of female isogeneic C3H mice (Taconic Farms, body weight 20–25 g) (Fu et al. 1984, Miura et al. 2004). To study the correlation between the copper and zinc analogues, biodistribution studies were carried out in mice with dorsal thoracic sc tumors (Table I). For human malignant glioma U373 cells, 5×10^6 cells (de Ridder et al. 1987) were implanted sc into the dorsal thorax of each recipient SCID/beige mouse (Taconic Farms) then studied when the tumors grew to at least 100 mm^3. All protocols involving the use of mice were approved by the Brookhaven National Laboratory (BNL) and the University of Connecticut Health Center (UCHC) animal care committees.

Table I. Average concentrations (and standard deviations) of boron (µg/g) in various tissues from BALB/c mice bearing subcutaneous EMT-6 mammary carcinomas, which were given either CuTCPH at 180 mg/kgbw or ZnTCPH at 210 mg/kgbw in 6 ip injections given over a period of 2 days then euthanized 2 or 4 days after the last injection.

Porphyrin	CuTCPH	ZnTCPH	CuTCPH	ZnTCPH
Time after last injection (d)	2	2	4	4
Number of mice	7	5	7	5
Tumor boron	62 ± 10	137 ± 59	71 ± 19	84 ± 21
Blood boron	0 ± 0.1	0.1 ± 0.1	0.3 ± 0.1	0.1 ± 0.1
Cerebrum boron	0.2 ± 0.1	0.2 ± 0.1	0.7 ± 0.3	0.3 ± 0.1
Pinna (mainly skin) boron	8.4 ± 2.1	7.2 ± 2.8	14.2 ± 2.6	5.9 ± 2.4
Liver boron	562 ± 79	555 ± 139	534 ± 124	501 ± 72
Tumor mass (mg)	405 ± 151	145 ± 93	335 ± 157	344 ± 174

Porphyrin administration

Each porphyrin was delivered in six injections: Three intraperitoneal (ip) injections at 4 h intervals over 8 h on two successive days. Injections of CuTCPH or ZnTCPH were begun in BALB/c mice when their EMT-6 tumors weighed ~100 mg (10–11 days after implantation): A total of 180–210 mg porphyrin/kilogram body weight (kgbw) was delivered in 0.01 ml/gram body weight (gbw)/injection. Similar injections were begun in SCID mice 32 days after their U373 tumors had been initiated (180–190 mg porphyrin/kgbw) and in C3H mice bearing ~100 mg SCCVII tumors (10 days post implantation, 350 mg porphyrin/kgbw). Mice were euthanized 2 or 4 days after the last injection then promptly necropsied. One mouse each from the CuTCPH and ZnTCPH groups was photographed in fluorescent and long-wave 'black' ultraviolet light before necropsy (Figure 1).

Histology

Cryotome (Thermo Scientific, Waltham, MA, USA) sections (~5 micrometer [μm]- or ~25 μm-thick) were prepared from tumor and liver tissue samples that had been snap-frozen in liquid-nitrogen-cooled isopentane immediately after euthanasia. Adjacent cryotome slices (~5 μm-thick) were mounted on 1″×3″ borosilicate glass microscope slides (Fisher Scientific, Pittsburgh, PA, USA) and either air-dried then frozen at about −20°C or formalin-fixed. Some of the former were counterstained with quinolinium, 4-[3-(3-methyl-2 (3H)-benzothiazolylidene)-1-propenyl]-1-[3-(trimethylammonio)propyl]-diiodide (TO-PRO-3); Molecular Probes, Eugene, Oregon, USA) or 3,3′dioctadecycloxacarbocyanine perchlorate (DiO), Molecular Probes, Eugene, Oregon) to highlight cell nuclei or cell cytoplasm, respectively. The latter were stained with hematoxylin/eosin at ambient room temperature.

Confocal fluorescence microscopy (CFM)

Cryotome sections of snap-frozen liver and tumor specimens were thawed on microscope slides, immediately overlaid with 2–5 μl phosphate-buffered saline (PBS), then sealed watertight with petroleum jelly under a borosilicate glass coverslip. Within minutes thereafter they were illuminated at 468 or 488 nanometer (nm) to image ZnTCPH's red fluorescence at 575–640 nm by CFM using either a model Zeiss LSM 410 or 510 instrument (Thornwood, NY, USA). To assess the sensitivity of the CFM system, normal BALB/c mice were injected ip as described above using progressively larger total doses of ZnTCPH (44, 87, or 174 mg/kgbw) and euthanized 2 days after the last injection. Cryotome sections of their livers (with correspondingly higher average concentrations of boron: 38, 89, or 168 μg/g) were examined by CFM without counterstaining at low magnification (Example: Figure 2, Frame A, average boron concentration, 38 μg/g wet liver). To visualize nuclei, a 1 mM stock solution of TO-PRO-3 was diluted 1:1000 in PBS then applied to the

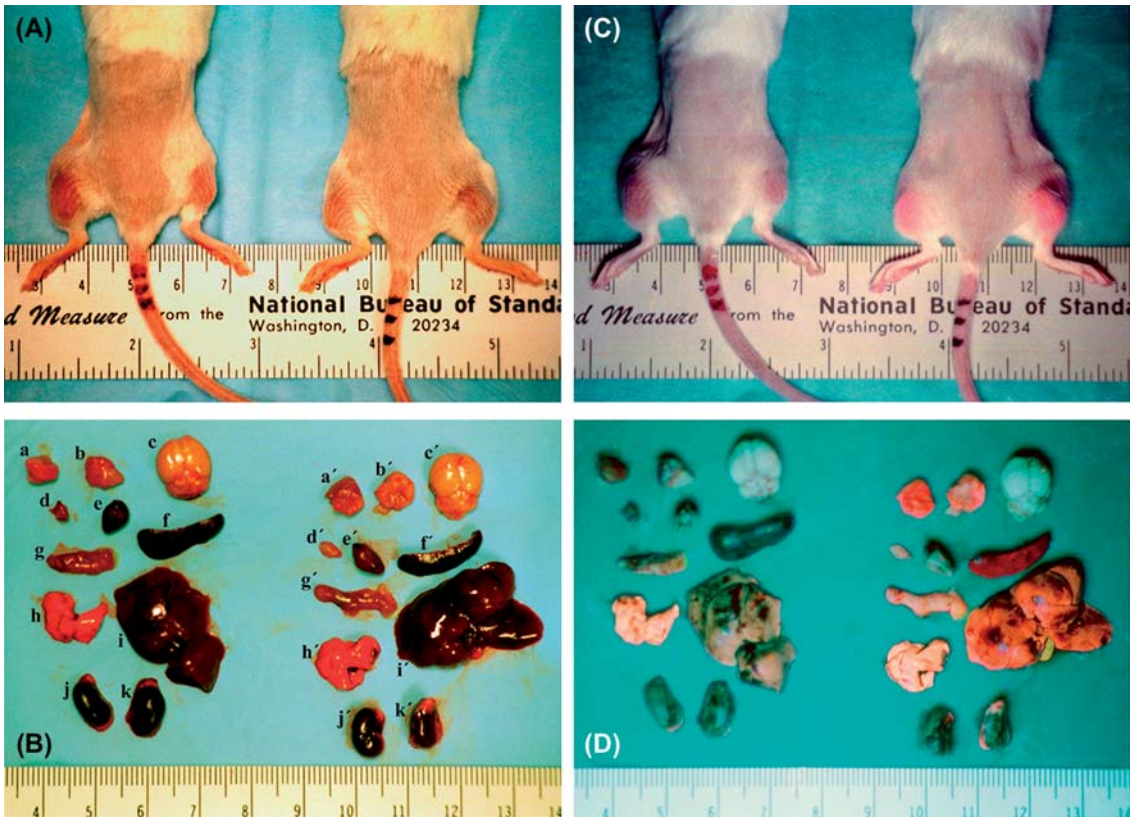

Figure 1. Mice with bilateral subcutaneous EMT-6 thigh tumors (A & C) and their organs (B & D) two days after the last of six intraperitoneal injections over two days of CuTCPH (left side of each frame) or ZnTCPH (right side of each frame): Illumination by standard 'fluorescent' ceiling light (A & B); illumination by long-wave ultraviolet ('black') light (C & D). The 11 pairs of letters, a, a′ through k, k′, label the left and right EMT-6 thigh tumors, brain, thymus, heart, spleen, duodenum, lungs, liver, and left and right kidneys from the CuTCPH-injected (left) and ZnTCPH-injected (right) mouse, respectively.

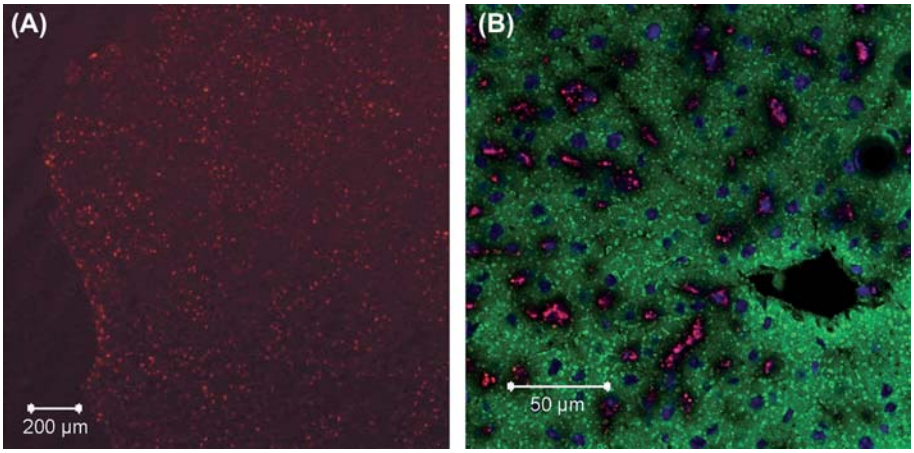

Figure 2. (A) Microdistribution of ZnTCPH in a cryostat section of a snap-frozen liver specimen from a normal BALB/C mouse injected with 44 mg/kgbw ZnTCPH that contained 38 μg/g B and examined by CFM at low magnification. (B) Microdistribution of ZnTCPH in a DiO-counterstained section of snap-frozen liver specimen from a similar mouse injected with 175 mg/kgbw that contained 108 μg/g B examined by CFM at higher magnification. This Figure is reproduced in color in the online version of International Journal of Radiation Biology.

thawed tissue section, which was illuminated at 633 nm. Its 'far-red' fluorescence was detected with a long-pass 650 nm filter and instantly computer-converted to blue in the image to avoid confusion with near-red ZnTCPH fluorescence. To visualize cytoplasm, a stock ethanolic solution (0.5 mM) of the lipophilic membrane dye DiO was diluted 1:100 in phosphate buffer solution (PBS), then applied to the thawed section; it was excited at 484 nm and its 501 nm fluorescence showed cells with green cytoplasmic features.

Boron analyses

Tissue samples (50–130 mg) were digested at 60°C with sulfuric acid:nitric acid (1:1). Triton X-100 and water were added to give final concentrations of ~50 mg tissue/ml with 15% total acid v/v and 5% Triton X-100 volume per volume (v/v). Direct current plasma atomic-emission spectroscopy (DCP-AES) with a detection limit of 0.1 μg B/ml sample homogenate was implemented with an Applied Research Laboratories (ARL) Fisons Model SS-7 instrument (Thermo-Optek, Franklin, MA, USA) (Barth et al. 1991).

Results

Visual biodistributions of CuTCPH and ZnTCPH in mice bearing EMT-6 tumors

Nominally similar doses of CuTCPH (190 mg/kgbw) or ZnTCPH (175 mg/kgbw) were injected ip into two BALB/c mice bearing bilateral EMT-6 thigh tumors. Four days after administration, the mice were euthanized and then photographed while illuminated, first by long-wave ultraviolet ('black') light (Figure 1C & D) for ~1 min, then under a standard indoor office 'fluorescent' ceiling light fixture for ~1 sec (Figure 1A & B). Red fluorescence was seen only from the ZnTCPH-injected mouse (Figure 1C, right). It was faint from the skin overall, but intense through the skin over the tumors. Strong red fluorescence from their organs removed at necropsy was visible only from the tumors, the liver, and the spleen of the ZnTCPH-injected mouse (Figure 1D, right); most organs from the CuTCPH-injected mouse appeared similar to those from the non-injected mice. In the absence of red fluorescence, green autofluorescence was seen from all tissues except the lungs (Figure 1D, right and left). DCP-AES assays showed higher concentrations of boron in liver and tumor samples removed from the CuTCPH-injected (Figure 1, left) mouse (~513 and ~98 μgB/g, respectively) than from the ZnTCPH-injected (Figure 1, right) mouse (~185 and ~34 μgB/g, respectively). This supports our hypothesis that CuTCPH, non-fluorescent in vitro, probably is not converted to a fluorescent metabolite in vivo.

Macroscopic biodistribution of boron in mice

Mice injected with similar doses of CuTCPH and ZnTCPH generally showed good correspondence in median boron concentrations, 68 vs. 88 μg B/g, respectively, in subcutaneous EMT-6 tumors of comparable median weights, 311 vs. 327 mg, respectively (Table I). When tumor sizes were dissimilar, average boron concentrations tended to be higher in the smaller tumors, as seen previously (Miura et al. 1992). Average liver boron levels, indicators of the concomitant bio availability of injected porphyrins to other tissues, were higher than those in tumor and changed in parallel with the latter from day 2–4 (Table I).

Microscopic distribution of ZnTCPH in liver

Fluorescence of ZnTCPH was barely detected by CFM in non-counterstained sections of livers with average macroscopic boron concentrations of 38 μg/g liver, which is therefore our rough estimate of the limit of detection in tissues of porphyrin-linked boron using the confocal microscopy technique described above (Figure 2A). Abundant cytoplasmic fluorescence from DiO-counterstained sections of snap-frozen liver specimens is depicted at higher magnification (Figure 2B). Its microscopic histological distribution suggests that most of the ZnTCPH in the liver is in hepatic macrophages (Kupffer cells), mainly in the periportal zones of the liver, with fluorescence practically absent from Kupffer cells in the centrilobular zones. These images, and others not shown, indicate

that virtually all the ZnTCPH was consistently excluded from nuclei of Kupffer cells and from virtually all of the hepatocytes. Little or none remained in extracellular compartments of the liver.

Microscopic distribution of ZnTCPH in subcutaneous tumors

The average (macroscopic) boron concentrations in the EMT-6, U-373 and SCCVII tumors shown in Figure 3, frames A, B, and C were 250, 115 and 110 μg/g following injections of 175–210, 180–190 and 350 mg porphyrin/kgbw, respectively. In A, virtually every identifiable cell nucleus (blue) is surrounded by a ring of reddish fluorescence attributable to ZnTCPH. In C, only some nuclei are associated with ZnTCPH fluorescence. Examination of these sections (and of many others not shown) indicates that ZnTCPH-derived fluorescence in tumors was only cytoplasmic and irregularly variable in distribution and intensity, unlike the repeatedly concentric lobular regularity of fluorescence seen microscopically by low-power magnification of liver sections. Further CFM images confirmed the cytoplasmic localization of ZnTCPH: Every zone of ZnTCPH fluorescence in a section of U-373 tumor (Figure 3B) was within a zone of DiO fluorescence visualized under different staining/optical filtration in a congruent section (Figure 3D), although the converse was not true. Our observations also showed that, in the EMT-6 and SCCVII tumors, almost every zone of tumor had some cells with finely punctate cytoplasmic fluorescence compatible with an origin in ZnTCPH-loaded organelles. However, the U373 tumor, which originated from a human glioblastoma, had only scattered zones of such fluorescence, which is compatible with focally occlusive endothelial hyperplasia associated with scattered infarction, which is characteristic of glioblastoma tissue.

Discussion

^{10}B-enriched CuTCPH-based BNCT was shown to be effective in locally controlling ~70% of EMT-6 carcinomas implanted in the thighs of mice using a porphyrin dose of 190 μg/gbw, which produced average tumor boron concentrations of 85 μg/g wet tissue (Miura et al. 2001). The average total radiation dose absorbed by tumor was 66 Gy, of which the beam only (i.e., boron-free) radiation dose was only 6 Gy. Similar tumor control was achieved using lower tumor doses (35–42 Gy) of 100 kVp X-rays, but with greater damage to the surrounding normal tissues (Miura et al. 2001). The compound biological effectiveness (CBE) factor is a weighting factor for the boron

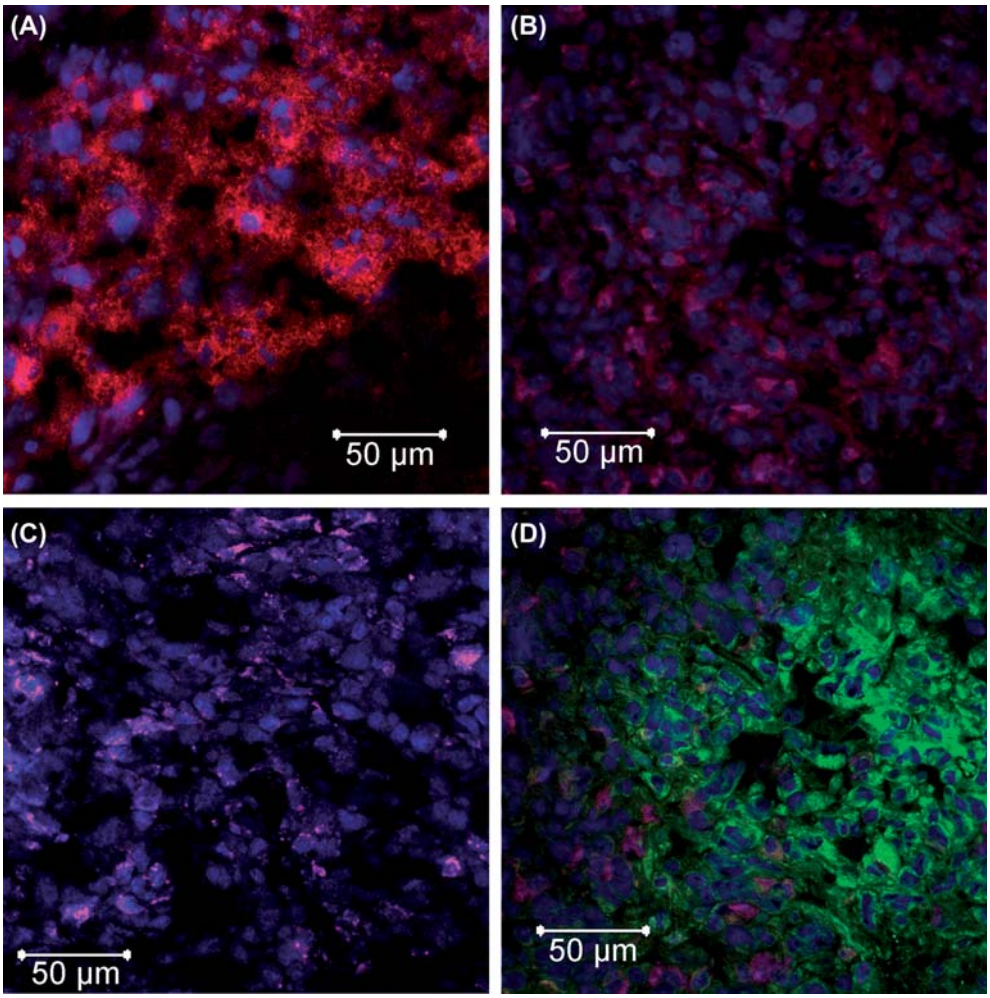

Figure 3. Microdistribution of ZnTCPH in TO-PRO-3-counterstained (for nuclei) sections of several malignant tumors: (A) A murine EMT-6 mammary carcinoma; (C) a murine SCCVII squamous cell carcinoma; (B & D) congruent sections of the U373 glioma. (D), counterstained with DiO for cytoplasm. This Figure is reproduced in color in the online version of International Journal of Radiation Biology.

neutron dose component in BNCT, a function of the RBE of the induced alpha particles and lithium ions modulated by the micro-distribution of the boron in the targeted tissues during irradiation. It can be considered analogous to the term relative biological effectiveness [RBE] weighting factor used for the other dose components in this mixed field irradiation (Morris et al. 1994). Because the absorbed radiation dose required to locally control EMT-6 tumors with X-rays is ~40 Gy and the total absorbed radiation dose using ^{10}B-CuTCPH-mediated BNCT for similar level of control is 66 Gy, it is speculated that the CBE factor for this tumor in this formulation is less than one (Miura et al. 2001). In contrast, the CBE factor for the BPA-fructose complex in a very different tumor model, rats bearing 9L gliosarcoms (in vivo irradiation with in vitro assay), was 1.2 or 1.5, depending on how it was injected (Morris et al. 2002). Moreover, a study using secondary ion mass spectroscopy (SIMS) in rat brain tissues indicated that BPA (shown by in vitro studies to be taken up into tumor cells via an amino acid transporter) is homogeneously distributed in rat gliosarcoma 9LGS cells throughout the cytoplasm and nucleus (Bennett et al. 1994). In contrast, the CFM images presented in this manuscript show that ZnTCPH is distributed heterogeneously throughout the cytoplasm (not the nucleus) of many, but not all EMT-6 carcinoma cells, which is consistent with its lower CBE factor.

The distribution patterns of ZnTCPH fluorescence in the cytoplasm of SCCVII and U373 subcutaneous tumors are similarly heterogeneous. Whether these porphyrins accumulated in the macrophages of these tumors (Kawabata et al. 2011b) as well as in their parenchymal cells was not determined in this study; low-magnification patterns of cell nuclei in the tumors suggested that the preponderance of cells were neoplastic. The preferential localization of the porphyrin in Kupffer cells rather than in hepatocytes in liver is consistent with observations of much lower toxicity from CuTCPH in mice than from some other porphyrins (Miura et al. 1996, 1998). Two days after administration of CuTCPH to mice, even at doses as high as 400 mg CuTCPH/kgbw, neither the weight losses nor the serum levels of hepatic enzymes alanine transaminase (ALT) and aspartate transaminase (AST) were significantly different from those in similar mice given excipient only (Miura et al. 2001), indicative of minimal or no hepatocellular toxicity. Although lipophilic porphyrin clearance is generally thought to be biliary, the green autofluorescence of the gallbladder (Figure 1D, right) suggests that little or none of the liver's ZnTCPH is excreted in the bile. This is consistent with the preferential localization of red fluorescence in Kupffer cells, with none evident in hepatocytes, the liver cells from which bile originates. That the fluorescence had a mainly portal distribution among Kupffer cells suggests that ZnTCPH was avidly removed from the blood during its first pass through the portal blood circulation, which is compatible with its intraperitoneal injection. If injected intravenously, we posit, a more uniform histologic distribution of red cytoplasmic fluorescence might be observed among Kupffer cells. No overt toxicity was evinced in mice injected by ZnTCPH or CuTCPH at any dose likely to be therapeutically relevant, but their toxicities were not studied past one week after injection (Miura et al. 2001). However, 4 months and one year after 400 mg CuTCPBr/kgbw was injected into normal BALB/c mice, there were no differences with regard to weight changes, platelet counts and liver enzyme concentrations between the CuTCPBr-injected mice and control mice concomitantly injected with excipient (M. Miura et al., unpublished data).

Compared with BPA, the boronated compound most often used currently for clinical BNCT, extraordinarily high average tumor concentrations of CuTCPH have been achieved. Our short-term studies show that doses of CuTCPH up to 400 mg/kgbw are well tolerated in mice, but long-term studies are lacking. Based on the microdistribution revealed in this study of ZnTCPH, we suggest that BNCT might be implemented more effectively by using a combination of a lipophilic porphyrin such as CuTCPH and a uniformly distributed ^{10}B-enriched agent such as BPA. BPA has less affinity than CuTCPH for the tumor types studied herein, but is relatively more uniformly distributed in two types of intracranial rat gliosarcomas (Smith et al. 2001). Since cytotoxic bystander effects (Kashino et al. 2009) extend the tumor-inhibiting effectiveness of radiation-induced free radicals beyond their scattered microscopic zones of origin in a tumor, BNCT based in part on a lipophilic porphyrin such as CuTCPH and in part on BPA might enable palliation of a wider variety of malignancies than is currently feasible; further studies are warranted.

CuTCPBr has been able to enhance the effects of X-irradiation of tumors in mice (Miura et al., 2012). It is expected that CuTCPH would not be as effective due to the lower reduction potential – i.e., from the lack of the electron withdrawing substituents on its macrocycle.

Conclusions

The fluorescent porphyrin ZnTCPH appears to be a useful experimental surrogate for CuTCPH, a potential boron carrier for BNCT. CFM of ZnTCPH indicated a heterogeneous distribution of porphyrin in tumor cells and a uniform one in liver. Preferential cytoplasmic localization of both porphyrins would largely explain why local control of mouse tumors required such high concentrations of CuTCPH-boron.

Acknowledgements

We gratefully acknowledge advice and assistance from Jason Kirk, Susan Krueger, Xiafeng Li, John H. Carson, and Michael S. Makar. We thank Dr Sara C. Rockwell and Dr J. Martin Brown for providing the EMT-6 and SCCVII cell lines, respectively. We are also grateful to the reviewers and editor for their helpful comments.

Declaration of interest

The authors report no conflicts of interest. The authors alone are responsible for the content and writing of the paper.

This work was supported by the Office of Biological and Environmental Research of the U.S. Department of Energy under Contract DE-AC02-98CH10986.

References

Barth RF, Adams DM, Soloway AH, Mechetner EB, Alam F, Anisuzzaman AK. 1991. Determination of boron in tissues and cells using direct-current plasma atomic emission spectroscopy. Analytical Chemistry 63:890–893.

Barth RF, Vicente MGH, Harling OK, Kiger WS, Riley KJ, Binns PJ, Wagner FM, Suzuki M, Aihara T, Kato I, Kawabata S. 2012. Current status of boron neutron capture therapy of high grade gliomas and recurrent head and neck cancer. Radiation Oncology 7:146.

Bennett BD, Mumford-Zisk J, Coderre JA, Morrison GH. 1994. Subcellular localization of p-boronophenylalanine-delivered boron-10 in the rat 9L gliosarcoma: Cryogenic preparation in vitro and in vivo. Radiation Research 140:72–78.

Chanana AD, Capala J, Chadha M, Coderre JA, Diaz AZ, Elowitz EH, Iwai J, Joel DD, Liu HB, Ma R, Pendzick N, Peress NS, Shady MS, Slatkin DN, Tyson GW, Wielopolski L. 1999. Boron neutron capture therapy for glioblastoma multiforme: Interim results from the phase I/II dose-escalation studies. Neurosurgery 44:1182–1193.

Coderre JA, Morris GM. 1999. The radiation biology of boron neutron-capture therapy. Radiation Research 151:1–18.

Cruickshank GS, Ngoga D, Detta A, Green S, James ND, Wojnecki C, Doran J, Hardie J, Chester M, Graham N, Ghani Z, Halbert G, Elliot M, Ford S, Braithwaite R, et al. 2009. A cancer research UK pharmacokinetic study of BPA-mannitol in patients with high grade glioma to optimise uptake parameters for clinical trials of BNCT. Applied Radiation and Isotopes 67(7–8 Suppl.):S1–2.

de Ridder LI, Laerum OD, Mark SJ. 1987. Invasiveness of human glioma cell lines in vitro: Relation to tumorigenicity in athymic mice. Acta Neuropathologica 72:207–213.

Fabris C, Vicente MG, Hao E, Friso E, Borsetto L, Jori G, Miotto G, Colautti P, Moro D, Esposito J, Ferretti A, Rossi CR, Nitti D, Sotti G, Soncin M. 2007. Tumor-locating and -photosensitising properties of meso-tetra(4-nido-carboranylphenyl)porphyrin (H2TCP). Journal of Photochemistry and Photobiology 89:131–138.

Fu KK, Rayner PA, Lam KN. 1984. Modification of the effects of continuous low dose rate irradiation by concurrent chemotherapy infusion. International Journal of Radiation Oncology Biology Physics 10:1473–1478.

Gabel D, Foster S, Fairchild RG. 1987. The Monte Carlo simulation of the biological effect of the 10B (n,alpha)7Li reaction in cells and tissue and its implication for boron neutron capture therapy. Radiation Research 111:14–25.

Haritz D, Gabel D, Huiskamp R. 1994. Clinical phase-I study of Na2B12H11SH (BSH) in patients with malignant glioma as precondition for boron neutron capture therapy (BNCT). International Journal of Radiation Oncology Biology Physics 28:1175–1181.

Henriksson R, Capala J, Michanek A, Lindahl SA, Salford LG, Franzen L, Blomquist E, Westlin JE, Bergenheim AT; Swedish Brain Tumor Group. 2008. Boron neutron capture therapy (BNCT) for glioblastoma multiforme: A phase II study evaluating a prolonged high-dose of boronophenylalanine (BPA). Radiotherapy and Oncology 88:183–191.

Hopf FR, Whitten DG. 1975. Photochemistry of porphyrins and metalloporphyrins. In: Smith K, editor. Poprhyrins and metalloporphyrins. New York: Elsevier. pp. 667–725.

Joel DD, Chadha M, Chanana AD, Coderre JA, Elowitz EH, Gebbers J-O, Liu HB, Micca PL, Nawrocky MM, Shady M, Slatkin DN. 1997. Uptake of BPA into glioblastoma multiforme correlates with tumor cellularity. In: Larsson B, Crawford J, Weinreich R, editors. Advances in neutron capture therapy, vol. II. Amsterdam: Elsevier. pp. 225–228.

Joensuu H, Kankaanranta L, Seppälä T, Auterinen I, Kallio M, Kulvik M, Laakso J, Vähätalo J, Kortesniemi M, Kotiluoto P, Serén T, Karila J, Brander A, Järviluoma E, Ryynänen P, et al. 2003. Boron neutron capture therapy of brain tumors: Clinical trials at the Finnish facility using boronophenylalanine. Journal of Neuro Oncology 62: 123–134.

Kankaanranta L, Seppälä T, Koivunoro H, Saarilahti K, Atula T, Collan J, Salli E, Kortesniemi M, Uusi-Simola J, Välimäki P, Mäkitie A, Seppänen M, Minn H, Revitzer H, Kouri M, et al. 2012. Boron neutron capture therapy in the treatment of locally recurred head and neck cancer: Final analysis of a phase I/II trial. International Journal of Radiation Oncology Biology Physics 82:e67–75.

Kashino G, Kondoh T, Nariyama N, Umetani K, Ohigashi T, Shinohara K, Kurihara A, Fukumoto M, Tanaka H, Muruhashi A, Suzuki M, Kinashi Y, Liu Y, Masunaga S, Watanabe M, et al. 2009. Induction of DNA double-strand breaks and cellular migration through bystander effects in cells irradiated with the slit-type microplanar beam of the SPring-8 synchrotron. International Journal of Radiation Oncology Biology Physics 74:229–236.

Kawabata S, Miyatake S, Hiramatsu R, Hirota Y, Miyata S, Takekita Y, Kuroiwa T, Kirihata M, Sakurai Y, Maruhashi A, Ono K. 2011a. Phase II clinical study of boron neutron capture therapy combined with X-ray radiotherapy/temozolomide in patients with newly diagnosed glioblastoma multiforme – study design and current status report. Applied Radiation and Isotopes 69:1796–1799.

Kawabata S, Yang W, Barth RF, Wu G, Huo T, Binns PJ, Riley KJ, Ongayi O, Gottumukkala V, Vicente MGH. 2011b. Convection enhanced delivery of carboranylporphyrins for neutron capture therapy of brain tumors. Journal of Neurooncology 103:175–185.

Miura M, Micca PL, Heinrichs JC, Gabel D, Fairchild RG, Slatkin DN. 1992. Biodistribution and toxicity of 2,4-divinyl-nido-o-carboranyldeuteroporphyrin IX in mice. Biochemical Pharmacology 43: 467–476. (1995. Erratum. Biochemical Pharmacology 50: 893–894.)

Miura M, Micca PL, Fisher CD, Heinrichs JC, Donaldson JA, Finkel GC, Slatkin DN. 1996. Synthesis of a nickel tetracarboranylphenylporphyrin for boron neutron-capture therapy: Biodistribution and toxicity in tumor-bearing mice. International Journal of Cancer 68:114–119.

Miura M, Micca PL, Fisher CD, Gordon CR, Heinrichs JS, Slatkin DN. 1998. Evaluation of carborane-containing porphyrins as tumour targeting agents for boron neutron capture therapy. British Journal of Radiology 71:773–781.

Miura M, Morris GM, Hopewell JW, Micca PL, Makar MS, Nawrocky MM, Renner MW. 2012. Enhancement of the radiation response of EMT-6 tumours by a copper octabromotetracarboranylphenyl porphyrin. British Journal of Radiology 85:443–450.

Miura M, Morris GM, Micca PL, Lombardo DT, Youngs KM, Kalef-Ezra JA, Hoch, DA, Slatkin DN, Ma R, Coderre JA. 2001. Boron neutron capture therapy of a murine mammary carcinoma using a lipophilic carboranyltetraphenylporphyrin. Radiation Research 155:603–610.

Miura M, Morris GM, Micca PL, Nawrocky MM, Makar MS, Cook SP, Slatkin DN. 2004. Synthesis of copper octabromotetracarboranylphenylporphyrin for boron neutron capture therapy and its toxicity and biodistribution in tumour-bearing mice. British Journal of Radiology 77:573–580.

Morris GM, Coderre JA, Hopewell JW, Micca PL, Rezvani M. 1994. Response of rat skin to boron neutron capture therapy with p-boronophenylalanine or borocaptate sodium. Radiotherapy and Oncology 39:253–259.

Morris GM, Micca PL, Nawrocky MM, Weissfloch LE, Coderre JA. 2002. Long-term infusions of p-boronophenylalanine for boron neutron capture therapy: Evaluation using rat brain tumor and spinal cord models. Radiation Research 158:743–752.

Ozawa T, Afzal J, Lamborn KR, Bollen AW, Bauer WF, Koo MS, Kahl SB, Deen DF. 2005. Toxicity, biodistribution, and convection-enhanced delivery of the boronated porphyrin BOPP in the 9L intracerebral rat glioma model. International Journal of Radiation Oncology Biology Physics 63:247–252.

Renner MW, Miura M, Easson MW, Vicente MG. 2006. Recent progress in the syntheses and biological evaluation of boronated porphyrins for boron neutron-capture therapy. Anti-Cancer Agents in Medicinal Chemistry 6:145–157.

Rockwell SC, Kallman RF, Fajardo LF. 1972. Characteristics of a serially transplanted mouse mammary tumor and its tissue culture adapted derivative. Journal of the National Cancer Institute 49:735–747.

Sköld K, H-Stenstam B, Diaz A-Z, Giusti V, Pelletteri L, Hopewell JW. 2010. Boron neutron capture therapy for glioblastoma multiforme: Advantage of prolonged infusion of BPA-f. Acta Neurologica Scandinavica 122:58–62.

Smith DR, Chandra S, Barth RF, Yang W, Joel DD, Coderre JA, 2001. Quantitative imaging and microlocalization of boron-10 in brain tumors and infiltrating tumor cells by SIMS ion microscopy: Relevance to neutron capture therapy. Cancer Research 61: 8179–8187.

Woodburn KW, Vardaxis NJ, Hill JS, Kaye AH, Phillips DR. 1991. Subcellular localization of porphyrins using confocal laser scanning microscopy. Photochemistry and Photobiology 54:725–732.

Yamamoto T, Nakai K, Matsumura, A. 2008. Boron neutron capture therapy for glioblastoma. Cancer Letters 262:143–152.

Zuk MM, Rihter BD, Kenney ME, Rodgers MA, Kreimer-Birnbaum M. 1994. Pharmacokinetic and tissue distribution studies of the photosensitizer bis(di-isobutyl octadecylsiloxy)silicon 2,3-naphthalocyanine (isoBOSINC) in normal and tumor-bearing rats. Photochemistry and Photobiology 59:66–72.